Structures of the Acyl−Enzyme Complexes of the *Staphylococcus aureus* β-Lactamase Mutant Glu166Asp:Asn170Gln with Benzylpenicillin and Cephaloridine[†,‡]

Celia C. H. Chen and Osnat Herzberg*

Center for Advanced Research in Biotechnology, University of Maryland Biotechnology Institute, 9600 Gudelsky Drive, Rockville, Maryland 20850, USA

Received September 28, 2000; Revised Manuscript Received December 5, 2000

ABSTRACT: The serine-β-lactamases hydrolyze β-lactam antibiotics in a reaction that proceeds via an acyl−enzyme intermediate. The double mutation, E166D:N170Q, of the class A enzyme from *Staphylococcus aureus* results in a protein incapable of deacylation. The crystal structure of this β-lactamase, determined at 2.3 Å resolution, shows that except for the mutation sites, the structure is very similar to that of the native protein. The crystal structures of two acyl−enzyme adducts, one with benzylpenicillin and the other with cephaloridine, have been determined at 1.76 and 1.86 Å resolution, respectively. Both acyl−enzymes show similar key features, with the carbonyl carbon atom of the cleaved β-lactam bond covalently bound to the side chain of the active site Ser70, and the carbonyl oxygen atom in an oxyanion hole. The thiadolizine ring of the cleaved penicillin is located in a slightly different position than the dihydrothiazine ring of cephaloridine. Consequently, the carboxylate moieties attached to the rings form different sets of interactions. The carboxylate group of benzylpenicillin interacts with the side chain of Gln237. The carboxylate group of cephaloridine is located between Arg244 and Lys234 side chains and also interacts with Ser235 hydroxyl group. The interactions of the cephaloridine resemble those seen in the structure of the acyl−enzyme of β-lactamase from *Escherichia coli* with benzylpenicillin. The side chains attached to the cleaved β-lactam rings of benzylpenicillin and cephaloridine are located in a similar position, which is different than the position observed in the *E. coli* benzylpenicillin acyl−enzyme complex. The three modes of binding do not show a trend that explains the preference for benzylpenicillin over cephaloridine in the class A β-lactamases. Rather, the conformational variation arises because cleavage of the β-lactam bond provides additional flexibility not available when the fused rings are intact. The structural information suggests that specificity is determined prior to the cleavage of the β-lactam ring, when the rigid fused rings of benzylpenicillin and cephaloridine each form different interactions with the active site.

The serine-β-lactamases, enzymes that confer bacterial resistance to β-lactam antibiotics, use a hydroxyl group of a serine residue [Ser70 in the class A consensus numbering scheme of Ambler et al. (*1*)] to degrade a wide range of β-lactam compounds. The nucleophilic hydroxyl group of the catalytic serine attacks the carbonyl carbon atom of the β-lactam bond of the antibiotic, in a reaction that leads to the formation of an acyl−enzyme intermediate. Next, a water molecule cleaves the acyl bond (*2*−*5*). This mechanism may be described schematically as follows:

$$E + S \overset{K_s}{\rightleftharpoons} ES \xrightarrow{k_2} EC \xrightarrow{k_3} E + P \qquad (1)$$

with E, S, and P representing the enzyme, substrate, and product, respectively; ES denotes the Michaelis complex, and EC denotes the acyl−enzyme complex.

β-lactamases exhibit wide variation in substrate specificity. In general, the class A serine β-lactamases are considered better penicillinases than cephalosporinases, although there are many exceptions to this rule. In the current study, structural differences between benzylpenicillin and cephaloridine interactions with β-lactamase from *Staphylococcus aureus* PC1 have been examined using recombinant enzyme (*6*). The enzyme hydrolyzes benzylpenicillin, a good substrate of the enzyme, at a steady-state rate of 120 s^{-1} and with K_m value of 10 μM. Cephaloridine, considered a rather poor substrate of the *S. aureus* enzyme, is hydrolyzed at an initial rate of 1.3 s^{-1} and a steady-state rate of 0.077 s^{-1} (*6*, *7*), although the K_m value of $<1\mu$M indicates good binding (*7*).

An invariant glutamic acid residue in the class A β-lactamases, Glu166, activates a proximal water molecule for nucleophilic attack on the acyl−enzyme intermediate (*8*, *9*). Mutant enzymes with Glu166 replaced by an uncharged residue are deacylation impaired, enabling the accumulation of stable acyl−enzyme complexes (*10*, *11*). For β-lactamase from *Escherichia coli*, a mutant enzyme of this type, E166N, was used to determine the crystal structure of a benzylpenicillin acyl−enzyme adduct (*12*). The identity of the hydro-

[†] Supported by the NIH Grant RO1-AI27175.

[‡] The coordinates of the crystal structures of E166D:N170Q β-lactamase in the unbound state and bound to benzylpenicillin and cephaloridine have been deposited in the Protein Data Bank (entry codes 1GHI, 1GHP, and 1GHM).

* To whom correspondence should be addressed (telephone, 301-738-6245; fax, 301-738-6255; e-mail, osnat@carb.nist.gov).

10.1021/bi002277h CCC: $20.00
Published on Web 01/31/2001

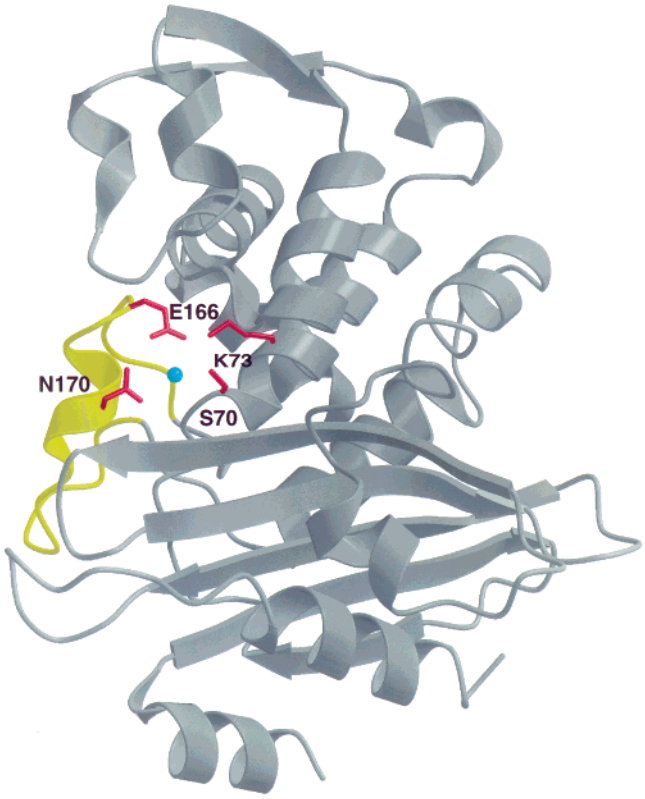

FIGURE 1: Overall fold of β-lactamase, highlighting the Ω-loop (gold), key active site residues, Ser70, Lys73, Glu166, and Asn170 (red), and the hydrolytic water molecule (blue).

lytic water molecule was confirmed by producing the mutant enzyme N170Q, with an extended side chain that blocks access to the water molecule and impairs deacylation (*13*).

Glu166 is located on an Ω-loop, comprising residues 163−178, that forms part of the active site depression (Figure 1). In the β-lactamase from *S. aureus* PC1, replacement of Glu166 by a glutamine residue, E166Q, yielded an enzyme that was deacylation impaired, but crystals could not be obtained (*14*). Thus, the double mutant enzyme, E166D:N170Q, was prepared. With this variant enzyme, the side chain of Gln170 blocks the site of the hydrolytic water molecule, and Asp166 should also reduce activity as the same mutation reduced the k_{cat} of the *Bacillus cereus* enzyme by approximately 3000-fold (*15*). The favorable electrostatic interaction between the catalytic Lys73 and residues 166 (now an aspartic acid) is still possible, and that may help preserve the conformational integrity of the Ω-loop, which is marginally stable in the β-lactamase from *S. aureus* (*16*, *17*). This rationale proved reasonable as the double replacement resulted in a deacylation-impaired enzyme, which crystallized readily.

The availability of crystals of E166D:N170Q β-lactamase facilitated the high-resolution structure determination of acyl−enzyme complexes with benzylpenicillin and with cephaloridine. The studies were undertaken to compare the binding mode of benzylpenicillin with the enzymes from *S. aureus* and from *E. coli* (*12*) and also to elucidate possible differences between the binding modes of benzylpenicillin and cephaloridine, two substrates with different kinetic parameters. The analysis indicates that the acyl−enzyme structures do not reflect the conformational constraints imposed on the intact antibiotic compound as it docks in the active site, and thus substrate specificity is not determined at the acyl−enzyme state.

MATERIALS AND METHODS

Mutagenesis, Expression, and Protein Purification. The E166D:N170Q β-lactamase from *S. aureus* PC1 was cloned, expressed in *E. coli* TG1, and purified following a similar protocol as in Zawadzke et al. (*6*), with modifications described in Zawadzke et al. (*13*). The pKK233-2-derived plasmid, pTS32, which exploits an IPTG-inducible *trc* promoter, was used to produce the mutant proteins. pTS32 contains the *S. aureus* β-lactamase gene (*bla*Z). It also contains a Tn9 chloramphenicol acetyl transferase gene, inserted into the TEM *bla*Z gene to prevent expression of the *E. coli* β-lactamase, and as a selectable marker of mutagenized genes. A N-terminal methionine has been added to the engineered gene for expression. The leader peptide of the β-lactamase was not included, and hence the first residue following the initiator methionine is Lys31. Mutations were introduced by the four-primer overlap-extension method (*18*). The altered *bla*Z genes were sequenced to confirm that the desired substitutions were obtained and that no spurious changes occurred.

The concentration of the purified protein was estimated from the absorbance of solutions at 280 nm by using the value of $\epsilon_{280} = 19\,500\ M^{-1}\ cm^{-1}$ (*19*). For storage, the protein was kept at 4 °C in solution containing 60% saturated ammonium sulfate.

Crystallization, β-Lactam Soaking Experiments, and X-ray Data Collection. Single crystals of β-lactamase were obtained at room temperature by vapor diffusion in hanging drops, using similar conditions to those used to obtain crystals of the native protein, with some modification. The protein drops were equilibrated against reservoir solutions containing 89% saturated ammonium sulfate, 0.5% PEG 2000, and buffered at pH 8 by 0.1 M sodium bicarbonate. The hanging drops contained equal volumes of 10 mg/mL enzyme and reservoir solutions. The crystals belong to space group *I*222 and are isomorphous with the native protein crystals. The unit cell dimensions for the E166D:N170Q mutant are $a = 54.0$ Å, $b = 93.8$ Å, $c = 139.3$ Å. There is one molecule in the asymmetric unit.

X-ray intensity data for the mutant protein crystal were collected at room temperature on a Siemens area detector mounted on a Siemens three-circle goniostat. Monochromatic Cu Kα X-rays were generated by a Siemens rotating anode. Data to 2.3 Å resolution were collected from a single crystal. The data were processed with the XENGEN package (*20*). The statistics of data processing are shown in Table 1.

For the binding studies, crystals were soaked for 17 h with 89% saturated ammonium sulfate solution containing 0.5 mM of either benzylpenicillin or cephaloridine, and buffered at pH 8.0 by 0.1 M sodium bicarbonate. The β-lactam solutions were replenished several times. Diffraction data were collected at 100 K. Each of the crystals to be frozen was coated with a layer of viscous oil (1:1 mixture of Paratone-N, Exxon, and mineral oil). The Oxford Cryostream was used for flash cooling. X-ray data were collected at the X12C beam line of the National Synchrotron Light Source (Brookhaven National Laboratory, Upton, NY). Diffraction intensities to 1.76 Å resolution for the benzylpenicillin-bound protein

Table 1: Data Processing Statistics[a]

	unbound	benzylpenicillin	cephaloridine
temp	room	100 K	100 K
wavelength (Å)	1.5414	1.15	1.00
cell dimen (Å)	54.0, 93.8, 139.3	52.9, 89.7, 138.8	53.5, 90.8, 140.2
resolution (Å)	2.3	1.76	1.80
no. of unique reflect.	15268 (2183)	29494 (2061)	31672 (3077)
completeness (%)	94.6 (83.0)	88.8 (63.0)	98.4 (96.9)
$\langle I/\sigma(I)\rangle$	7.6 (1.6)	17.9 (2.2)	16.7 (1.6)
R_{merge}[b]	0.121 (0.390)	0.053 (0.109)	0.045 (0.413)

[a] The values in parentheses correspond to the highest resolution shell. For the cephaloridine complex, refinement was carried out at 1.86 Å resolution. The total number of unique reflections at that resolution is 28595. $\langle I/\sigma(I)\rangle$ at the resolution shell between 1.94 and 1.86 Å is 2.8, and R_{merge} is 0.297. [b] $R_{merge} = \Sigma_h\Sigma_i |\langle I(h)\rangle - I(h)_i|/\Sigma_h\Sigma_i I(h)_i$ for equivalent observations.

crystal and to 1.80 Å resolution for the cephaloridine-bound protein crystal were recorded on a CCD-based detector (1-module Brandeis for the benzylpenicillin study and 4-module Brandeis for the cephaloridine study). Data acquisition was controlled with the computer program MADNES (*21*), driven by a graphical user interface (*22*). The data were processed and scaled with the computer program package HKL (*23*). Data statistics are shown in Table 1.

Structure Determination and Refinement. The crystals of the mutant enzyme at the unbound state were isomorphous with the native crystals. Hence, the starting model for refinement was that of the native *S. aureus* PC1 β-lactamase (PDB entry code 3BLM), except that the amino acid residues at positions 166 and 170 were truncated to alanine. The structure factors were scaled to absolute values with the computer program ORESTES written by W. E. Thiessen and H. A. Levy. The structure was refined with the program X-PLOR (*24*), including 11804 reflections in the resolution range 8.0−2.3 Å for which $F \geq 2\sigma(F)$. The positional and temperature factor refinement protocols were used.

The refinements of the two acyl−enzyme structures were also carried out with X-PLOR. That of the cephaloridine-bound protein was completed with CNS (*25*), including bulk solvent correction, and using maximum likelihood target function (*26*). The parent protein molecule was that of the S70A mutant structure refined at 120 K, as the flash-cooled crystals undergo a large change in the b cell dimension and are more similar to each other than to the crystals at room temperature. Residues 166 and 170 were truncated to alanines and later were replaced by Asp and Gln, respectively (*27*; PDB entry code 1DJC). Models for the benzylpenicillin and cephaloridine with cleaved β-lactam bonds were generated based on the intact compounds and the appropriate parameter and topology files constructed for the refinement. Because of the poor quality of the data for the cephaloridine-soaked crystal between 1.86 and 1.80 Å resolution (Table 1), the refinement was carried out at 1.86 Å resolution.

The progress of the refinement was evaluated by the improvement in the quality of the electron density maps and the reduced values of the conventional R factor ($R = \Sigma_h||F_o| - |F_c||/\Sigma_h|F_o|$, where $|F_o|$ and $|F_c|$ are the observed and calculated structure factor amplitudes, respectively) and the free R-factor (*28*).

The electron density maps were inspected and the models were modified on an interactive graphics workstation with the program TURBO-FRODO (*29*). Two types of electron density maps with the coefficients $2|F_o| - |F_c|$ and $|F_o| - |F_c|$, and with calculated phases were inspected simultaneously. Solvent molecules were added once the R-value was lower than 0.25. These were assigned in the $|F_o| - |F_c|$ difference Fourier maps with a 3σ cutoff level for inclusion in the model.

Table 2: Hydrolysis Rates for the Wild Type and G166D:N170Q β-Lactamases

substrate	protein	k_{cat} (s^{-1})	burst[a]
benzylpenicillin	wild type	120 ± 2[b]	
	E166D:N170Q	undetectable	undetectable
nitrocefin	wild type	11.4[c]	
	E166D:N170Q	0.0002 ± 0.0001	1

[a] The burst is the ratio [product]/[enzyme] obtained by extrapolating the line at the steady-state phase to time zero. [b] Taken from ref *6*. [c] Taken from ref *16*.

Enzyme Kinetics. Kinetic measurements were made on a Hewlett-Packard 8452A diode array spectrophotometer. Assays were performed at 25 °C in solutions containing 0.1 M potassium phosphate buffer at pH 6.8. The dependence of the nitrocefin kinetics on ammonium sulfate concentration was also evaluated.

Nitrocefin was purchased from Unipath (Ogdensburg, NY). Benzylpenicillin and cephaloridine were purchased from Sigma (St. Louis, MO). Hydrolysis of the chromogenic cephalosporin, nitrocefin, was monitored by the increase in absorbance at 500 nm ($\Delta\epsilon_{500} = 15\,900$ M^{-1} cm^{-1}). The hydrolysis of benzylpenicillin was monitored by loss of absorbance at 232 nm ($\Delta\epsilon_{232} = 940$ M^{-1} cm^{-1}).

RESULTS AND DISCUSSION

Enzyme Kinetics. The kinetics of E166D:N170Q β-lactamase shows that the deacylation catalytic machinery has been eliminated (Table 2). Benzylpenicillin hydrolysis is undetectable, and nitrocefin hydrolysis is close to the noise level of the spectrophotometer, at approximately 5.7×10^4 slower steady state rate than the hydrolysis by the wild-type enzyme. With the chromogenic substrate, nitrocefin, the absorption changes are sufficiently high to reveal a fast burst (within the dead time of the spectrophotometer) with stoichiometry of 1 mol of product/mol of enzyme, followed by a much slower steady-state phase. The burst corresponds to the formation of a stable acyl enzyme, assuming the same extinction coefficient for the acyl enzyme as that for the free hydrolyzed nitrocefin. The burst amplitude remained 1 when the assay was performed in solutions containing 15% saturated ammonium (~0.6 M). The independence of the burst magnitude of salt concentration is taken as evidence that the burst kinetics arises from the elimination of the enzyme machinery responsible for deacylation rather than because of protein conformational changes (*30*).

The formation of a stable acyl−enzyme with benzylpenicillin cannot be detected spectroscopically, because of the small changes in absorption associated with substrate hydrolysis and the large absorption of the protein at the wavelength where benzylpenicillin hydrolysis is monitored. However, preincubation of the mutant enzyme with 2-fold excess benzylpenicillin for 100 s eliminated any activity toward nitrocefin. This is consistent with the formation of a

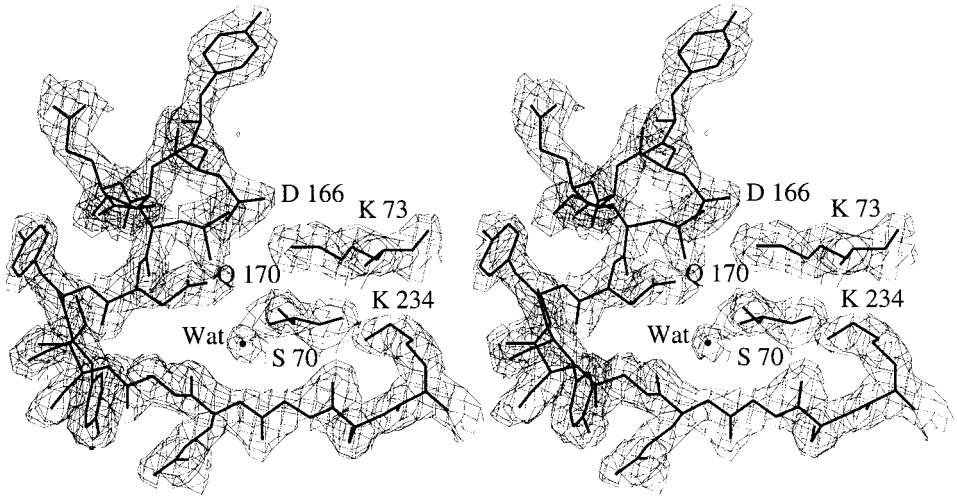

FIGURE 2: Stereoscopic representation of the active site electron density map of the N166D:N170Q β-lactamase. The coefficients $2F_o-F_c$ and calculated phases are used. The map is contoured at 1σ level.

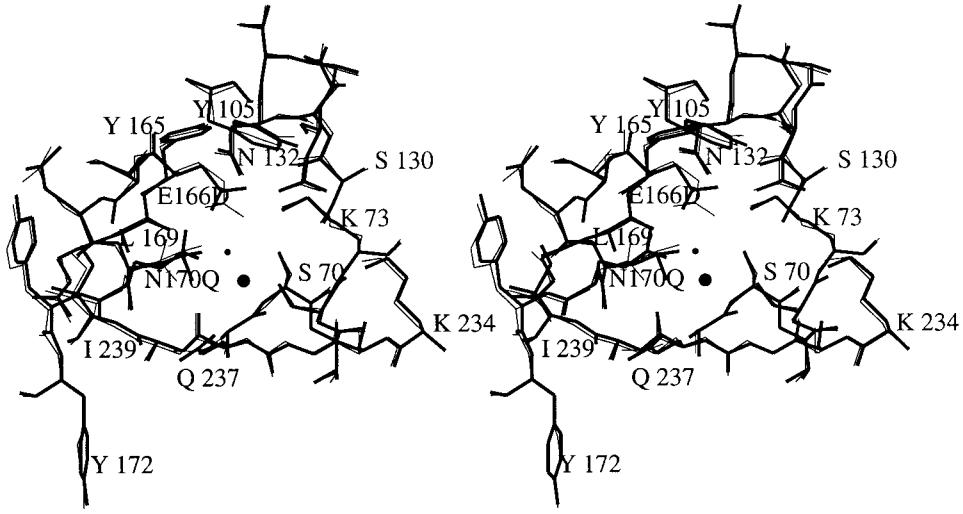

FIGURE 3: Superposition of the active site of native and E166D:N170Q β-lactamase. The native structure is shown in solid thin line and the mutant structure is shown in solid thick line. The water molecule in the oxyanion hole (present in both structures) is shown as a large circle, and the hydrolytic water molecule (not present in the mutant structure) is shown as a small circle. The carboxylate group of Asp166 interacts with Lys73 but is oriented differently than the carboxylate group of Glu166 in the native structure. The side chain of Gln170 blocks the site of the hydrolytic water molecule.

stable acyl−enzyme with benzylpenicillin, as indeed has been revealed by the crystallographic binding studies.

The Refined Crystal Structures. The final model of E166D:N170Q β-lactamase includes the 257 amino acid residues, a total of 138 water molecules, and a bicarbonate ion (the buffer in the crystallization solution was sodium bicarbonate). The final crystallographic *R*-factor for 11 804 reflections between 8.0 and 2.3 Å resolution for which $F \geq 2\sigma F$ is 0.153. The root-mean-square deviations (rmsd) from ideal bond length and bond angle values of the standard geometry compiled by Engh and Huber (*31*) are 0.020 Å and 2.1°, respectively. The electron density map in the vicinity of the active site is shown in Figure 2.

The overall fold of the mutant protein is the same as that of the native protein, with rmsd between α-carbon atom positions of 0.2 Å. The two replaced residues have not altered the active site architecture significantly (Figure 3). The changes are localized at the mutation sites. Asp166 still forms an ion pair with the catalytic residue Lys73 (3.1 Å), as does Glu166 in the native structure, but the side chain orientation is different. Gln170 displaces the hydrolytic water molecule, as seen previously in the structure of the single mutant, N170Q β-lactamase (*13*). The bicarbonate ion is located in the same site as that of the sulfate in the E166Q:N170D enzyme structure (*14*). Although the concentration of sulfate is much higher than that of bicarbonate, the shape of the electron density here is planar, which is inconsistent with a tetrahedral sulfate ion. As observed in the native structure (*9*), a water molecule binds in the oxyanion hole formed between the main chain nitrogen atoms of Ser70 and Gln237.

The quality of the two acyl enzyme structures is better than that of the structure of the unbound protein, because the diffraction detected at the synchrotron extended to substantially higher resolution and because the data were collected at 100 K. The final model of the benzylpenicillin-bound enzyme includes the 257 amino acid residues, the benzylpenicillin with the cleaved β-lactam bond covalently bound to Ser70, 4 sulfate ions, and 385 water molecules. The loop region comprising residues 194−199, located 20 Å away from the active site, has been modeled with two

alternate conformations. The ability to identify these two alternate conformations is attributed to the high resolution of the diffraction data. In addition, side chains of four lysine residues, two isoleucine residues, and one methionine have been modeled with two alternate conformations, and 9 water molecules have each been modeled with two alternate positions. The final crystallographic *R*-factor for 25 528 reflections at the resolution between 8.0 and 1.76 Å for which $F \geq 2\sigma(F)$ is 0.185 and the free *R* is 0.264 (for 10% of the data not included in the refinement). The rmsd from ideal bond length and bond angle values of the standard geometry are 0.017 Å and 1.9°, respectively.

The model of the cephaloridine-bound β-lactamase mutant includes 257 amino acid residues, the covalently bound cephaloridine with cleaved β-lactam bond and without the leaving group at position C(3), five sulfate ions, one bicarbonate ion, and 327 water molecules. The positions of the four sulfate ions in the benzylpenicillin complex structure overlap with the positions of three of the sulfate ions and the bicarbonate ion in the cephaloridine complex. The final crystallographic *R*-factor for 24 212 reflections at the resolution between 8.0 and 1.86 Å for which $F \geq 2\sigma(F)$ is 0.188 and the free *R* is 0.241 (10% of the data not included in the refinement). The rmsd from ideal bond length and bond angle values of the standard geometry are 0.020 Å and 1.9°, respectively.

Figure 4 shows the electron density associated with the bound benzylpenicillin and cephaloridine.

Structural Basis for Impaired Hydrolysis. The mutant E166D:N170Q retains a carboxylate group at a position close enough to form a salt bridge with Lys73. The impaired deacylation is attributed mainly to the side chain of Gln170 blocking the hydrolytic water site, as reported previously for the single mutant enzyme N170Q (*13*). In addition, the orientation of the carboxylate group of Asp166 differs from that of Glu166 in the wild-type enzyme. Even if a water molecule could occasionally displace Gln170 and bind in the right position for hydrolyzing the acyl enzyme, the disposition of Asp166 carboxylate group may be inappropriate for enhancing the nucleophilicity of the water molecule (Figure 3).

The β-Lactam Acyl−Enzyme Complexes. The protein structure changes very little upon binding of either β-lactam compound (Figure 5, panels a−c). The three most notable changes are (i) The side chain of the mutated residue, Gln170, adopts an alternate conformation to avoid short contacts with the side chain attached to C(6) or C(7) position of the cleaved β-lactam rings of benzylpenicillin and cephaloridine, respectively. (ii) The χ_4 dihedral angle of Lys73 changes slightly, leading to an increased distance between the mutated residue, Asp166, and Lys73 from 3.1 Å in the unbound state to 4.1 and 3.9 Å in the benzylpenicillin and cephaloridine-bound structures, respectively. This movement of Lys73 also leads to a new interaction between the amino group of Lys73 and the hydroxyl oxygen atom of Ser130 (2.9 and 3.2 Å for the benzylpenicillin and cephaloridine acyl enzymes, respectively), in contrast to the longer distance seen in the unbound state (4.2 Å). The position of Asp166 side chain does not change though, and its interactions with the side chain of Gln170, with the side chain of the core residue, Asn135, and with an internal water molecule are maintained. (iii) The side chain of Tyr105 adopts an

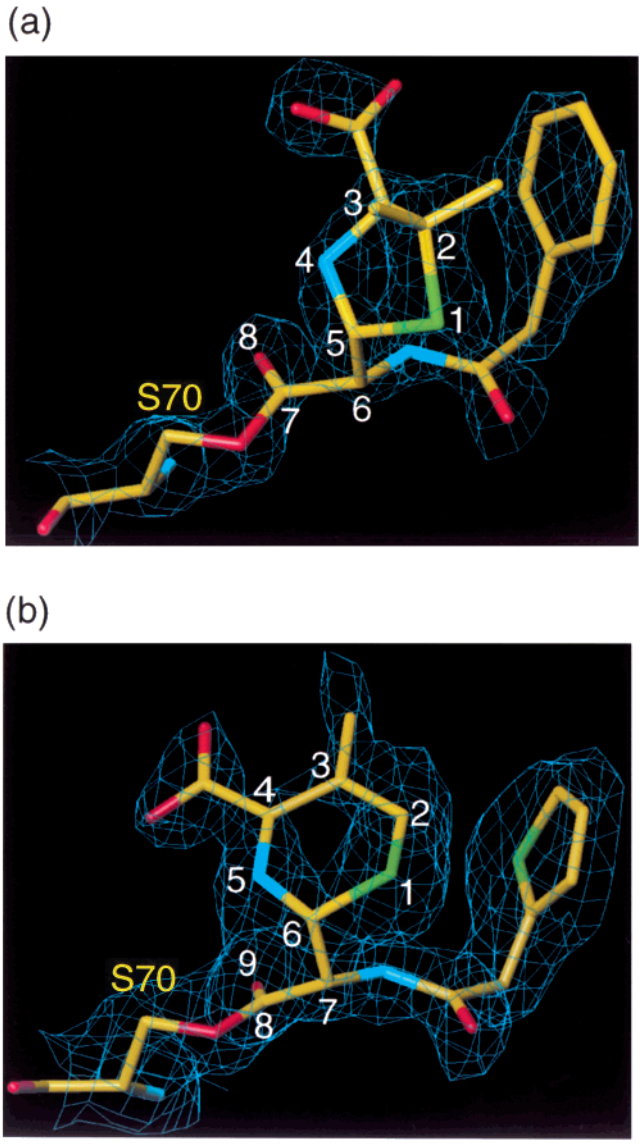

FIGURE 4: The electron density associated with the bound β-lactam antibiotics. The density from the hydroxyl group of Ser70 extends continuously to the β-lactams, confirming the formation of covalently bound adducts. Atoms of the cleaved antibiotic's nucleus are numbered. (a) Benzylpenicillin; (b) cephaloridine.

alternate conformation to that seen in the unbound state. The same change was observed earlier in the structure of the complex with a phosphonate inhibitor, a tetrahedral transition state analogue (*32*). The change leads to edge to face interaction between the aromatic ring of Tyr105 and the aromatic ring of the substrate/inhibitor. Note that the same change occurred also in the structure of the free enzyme determined at 120 K (*33*). In that case, the altered conformation is attributed to a ∼7% reduction in one of the unit cell dimension due to the flash-cooling, leading to a short intermolecular contact between two Tyr105 hydroxyl groups related by crystallographic 2-fold symmetry axis.

The two antibiotic compounds, benzylpenicillin and cephaloridine, bind to the enzyme in a similar manner (Figure 5, panels b−d). The carbonyl carbon of the cleaved β-lactam ring is covalently bonded to the hydroxyl group of Ser70, forming an ester bond. The carbonyl oxygen atom of the cleaved β-lactam ring is located in the oxyanion hole formed by the backbone amide groups of Ser70 and Gln237, with

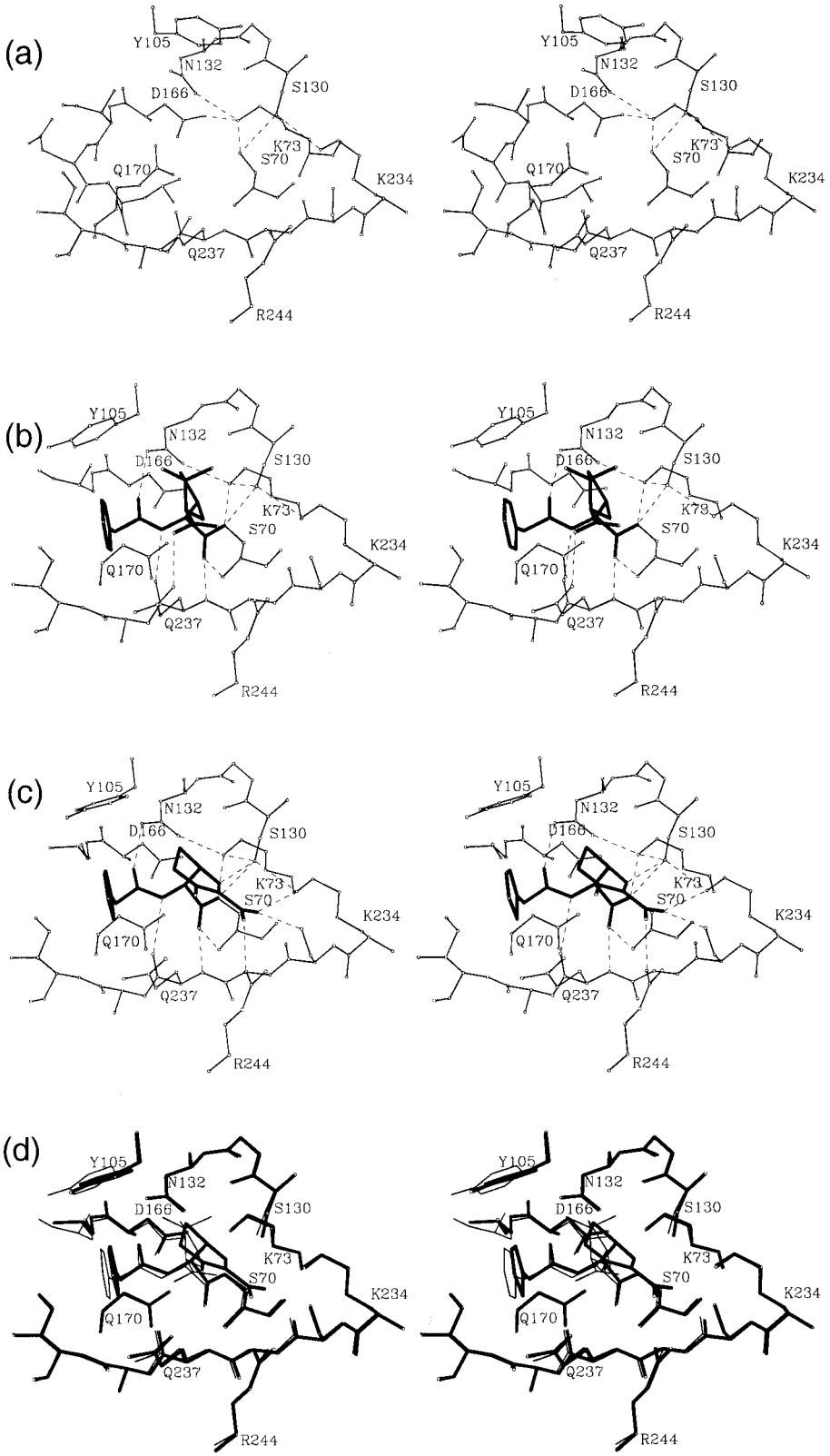

FIGURE 5: Stereoscopic representation of the active site of E166D:N170Q β-lactamase in the (a) unbound state, (b) bound to benzylpenicillin, (c) bound to cephaloridine, (d) superposition of the active site residues and the two β-lactam compounds. In panels a−c: protein residues − solid thin line; β-lactam − solid thick line. Key interactions between protein groups and between the protein and the antibiotics are highlighted in broken lines. In panel d, the acyl enzyme with benzylpenicillin is shown in solid thin line and with cephaloridine in solid thick line.

oxygen−nitrogen atom distances varying between 2.7 and 3.0 Å. The side chain attached to the cleaved β-lactam rings at position C(6) for benzylpenicillin and position C(7) for cephaloridine consists of a peptide group followed by a CH_2 group and an aromatic ring. For both substrates, this side chain is oriented similarly toward the Ω-loop, with the amide nitrogen atom interacting with the backbone carbonyl group of Gln237, and the carbonyl group interacting with the side

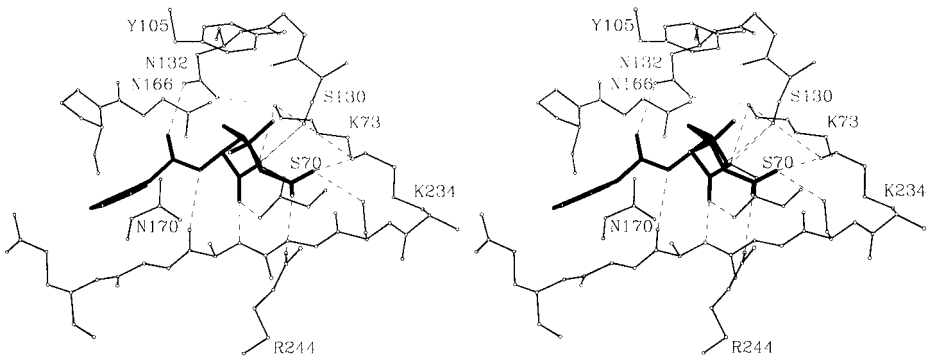

FIGURE 6: Stereoscopic representation of the active site of *E. coli* E166N β-lactamase acyl enzyme with benzylpenicillin in the same orientation to that shown in Figure 5. Protein residues − solid thin line; β-lactam − solid thick line. Key interactions between the protein groups and between the protein and the antibiotics are highlighted in broken lines.

chain of Asn132. The aromatic moiety of the β-lactam side chain substituent (benzyl group in benzylpenicillin, and theinyl group in cephaloridine) is surrounded by hydrophobic residues. In addition to the edge to face interaction with the side chain of Tyr105, there are also interactions with the side chains of Ile239 and Ile167.

The side chain attached to the dihydrothiazine ring of cephaloridine at position C(3) is not seen in the electron density map, consistent with the suggestion that a nucleophilic attack on the β-lactam carbonyl carbon is concerted with departure of the leaving group at C(3) (*34*).

The thiadolizine ring of benzylpenicillin and the dihydrothiazine ring of cephaloridine are located in slightly different positions. Consequently, the carboxylate moieties attached to the rings are oriented differently and form different sets of interactions. In benzylpenicillin, the carboxylate group forms an electrostatic interaction with the side chain of Gln237 (2.9 Å) and is oriented toward solvent. In cephaloridine, the carboxylate group is more shielded from solvent by intricate interactions with the guanidinium group of Arg244 (2.7 Å), the hydroxyl group of Ser235 (2.6 Å), and the amino group of Lys234 (3.4 Å). The position of the carboxylate group of cephaloridine is similar to that of the bicarbonate ion seen in the active site of the unbound mutant structure. There is no obvious reason for the different positions of the thiadolizine and the dihydrothiazine and their respective carboxylate groups. Indeed, modeling shows that both positions may be adopted by either compound, except for a somewhat close contact between the sulfur atom of the dihydrothiazine and the carbonyl oxygen of Ser130, when adopting the conformation seen with the benzylpenicillin.

The comparison between the two acyl−enzymes does not reveal structural features that could account for the more rapid rate of hydrolysis of benzylpenicillin as compared with cephaloridine by wild-type β-lactamase. Moreover, the hydrolytic water molecule present when position 170 is occupied by the native asparagine is equally well positioned for nucleophilic attack on the carbonyl carbon atom of either cleaved β-lactam antibiotics. The relative activity must therefore be determined prior to acyl−enzyme formation. That is, when the fused rings of the antibiotics are intact, productive binding requires that the carbonyl carbon of the β-lactam ring is poised for nucleophilic attack by the hydroxyl group of Ser70, while the carboxylate group interacts with Lys234. Apparently, the structural framework of the active site is better suited to accommodate these groups in the context of benzylpenicillin as compared with cephaloridine.

Comparison with the E. coli β-Lactamase Acyl−Enzyme. The key interactions described above were also observed in the *E. coli* β-lactamase−benzylpenicillin acyl−enzyme structure (*12*). However, the mode of binding observed for the *E. coli* acylenzyme is more similar to that of the *S. aureus* β-lactamase−cephaloridine complex. The location of the respective β-lactam carboxylate moieties is the same (Figure 6). This further illustrates the additional conformational flexibility of β-lactam compounds once the β-lactam bond has been cleaved. A feature differentiating the *S. aureus* and *E. coli* acyl−enzymes is the orientation of the aromatic groups of the β-lactam side chain substituents. In the two *S. aureus* acyl−enzymes, they are oriented perpendicular to the β-lactam aromatic ring seen in the *E. coli* acyl−enzyme. The structural rationale is obvious: The *S. aureus* enzyme contains an isoleucine at position 239, which constitutes an insertion as compared with the amino acid sequence of the *E. coli* enzyme (Figure 5). The aromatic ring of the β-lactam would form short contacts with Ile239 if it adopted the conformation seen in the *E. coli* acyl−enzyme, whereas it actually forms a favorable hydrophobic interaction with Ile239 in the perpendicular orientation. Interestingly, Tyr105 of *S. aureus* β-lactamase acyl−enzymes adopts an alternate conformation to that seen in the unbound state, which enables edge to face interactions with the β-lactam aromatic ring. In contrast, the location of the β-lactam aromatic ring in the *E. coli* acyl−enzyme structure is too remote from Tyr105, and the conformation of Tyr105 side chain remains the same as in the unbound state.

ACKNOWLEDGMENT

We thank Drs. Robert Sweet, John Skinner, and Salvatore Sclafani at the National Synchrotron Light Source (Brookhaven National Laboratory, Upton, NY) for help and advice in data collection and data processing. We thank Drs. Kui Huang and Soojay Banerjee for sharing the load of data collection in Brookhaven.

REFERENCES

1. Ambler, R. P., Coulson, A. F., Frere, J. M., Ghuysen, J. M., Joris, B., Forsman, M., Levesque, R. C., Tiraby, G., and Waley, S. G. (1991) *Biochem. J. 276*, 269−70.
2. Knott-Hunziker, V., Waley, S. G., Orlek, B. S., and Sammes, P. G. (1979) *FEBS Lett. 99*, 59−61.

3. Cartwright, S. J., and Coulson, A. F. (1980) *Philos. Trans. R. Soc. Lond. B Biol. Sci. 289*, 370−2.
4. Cohen, S. A., and Pratt, R. F. (1980) *Biochemistry 19*, 3996−4003.
5. Fisher, J., Charnas, R. L., Bradley, S. M., and Knowles, J. R. (1981) *Biochemistry 20*, 2726−31.
6. Zawadzke, L. E., Smith, T. J., and Herzberg, O. (1995) *Protein Eng. 8*, 1275−85.
7. Faraci, W. S., and Pratt, R. F. (1985) *Biochemistry 24*, 903−10.
8. Herzberg, O., and Moult, J. (1987) *Science 236*, 694−701.
9. Herzberg, O. (1991) *J. Mol. Biol. 217*, 701−19.
10. Escobar, W. A., Tan, A. K., and Fink, A. L. (1991) *Biochemistry 30*, 10783−7.
11. Adachi, H., Ohta, T., and Matsuzawa, H. (1991) *J. Biol. Chem. 266*, 3186−91.
12. Strynadka, N. C., Adachi, H., Jensen, S. E., Johns, K., Sielecki, A., Betzel, C., Sutoh, K., and James, M. N. (1992) *Nature 359*, 700−5.
13. Zawadzke, L. E., Chen, C. C., Banerjee, S., Li, Z., Wasch, S., Kapadia, G., Moult, J., and Herzberg, O. (1996) *Biochemistry 35*, 16475−82.
14. Chen, C. C., and Herzberg, O. (1999) *Protein Eng. 12*, 573−9.
15. Gibson, R. M., Christensen, H., and Waley, S. G. (1990) *Biochem. J. 272*, 613−9.
16. Herzberg, O., Kapadia, G., Blanco, B., Smith, T. S., and Coulson, A. (1991) *Biochemistry 30*, 9503−9.
17. Banerjee, S., Shigematsu, N., Pannell, L. K., Ruvinov, S., Orban, J., Schwarz, F., and Herzberg, O. (1997) *Biochemistry 36*, 10857−66.
18. Ho, S. N., Hunt, H. D., Horton, R. M., Pullen, J. K., and Pease, L. R. (1989) *Gene 77*, 51−9.
19. Carrey, E. A., and Pain, R. H. (1978) *Biochim. Biophys. Acta 533*, 12−22.
20. Howard, A. J., Gilliland, G. L., Finzel, B. C., Poulos, T., Ohlendorf, D. O., and Salemme, F. R. (1987) *J. Appl. Cryst. 20*, 383−7.
21. Messerschmidt, A., and Pflugrath, J. W. (1987) *J. Appl. Crystallogr. 20*, 306−15.
22. Sweet, R. M., and Skinner, J. (1995) in *American Crystallographic Association Annual Meetings Abstracts*, pp 1a.7.A.42.
23. Otwinowski, Z., and Minor, W. (1997) *Methods Enzymol. 276*, 538−56.
24. Brünger, A. T. (1992) Yale University Press, New Haven and London.
25. Brünger, A. T., Adams, P. D., Clore, G. M., DeLano, W. L., Gros, P., Grosse-Kunstleve, R. W., Jiang, J. S., Kuszewski, J., Nilges, M., Pannu, N. S., Read, R. J., Rice, L. M., Simonson, T., and Warren, G. L. (1998) *Acta Crystallogr. D Biol. Crystallogr. 54*, 905−21.
26. Pannu, N. S., Read, R. J. (1996) *Acta Crystallogr. A52*, 659−668.
27. Chen, C. C., Smith, T. J., Kapadia, G., Wasch, S., Zawadzke, L. E., Coulson, A., and Herzberg, O. (1996) *Biochemistry 35*, 12251−8.
28. Brünger, A. T. (1992) *Nature 355*, 472−474.
29. Roussel, A., and Cambillau, C. (1989) Silicon Graphics, Mountain View, CA.
30. Banerjee, S., Pieper, U., Kapadia, G., Pannell, L. K., and Herzberg, O. (1998) *Biochemistry 37*, 3286−96.
31. Engh, R. A., and Huber, R. (1991) *Acta Cryst. A47*, 436−52.
32. Chen, C. C., Rahil, J., Pratt, R. F., and Herzberg, O. (1993) *J. Mol. Biol. 234*, 165−78.
33. Chen, C. C., and Herzberg, O. (1992) *J. Mol. Biol. 224*, 1103−13.
34. Page, M. I. (1987) *Adv. Phys. Org. Chem. 23*, 165−269.

BI002277H